Published paper:

Keim, DM, West, LJ and Odling, NE (2012) *Convergent Flow in Unsaturated Fractured Chalk.* Vadose Zone Journal, 11 (4).

http://dx.doi.org/10.2136/vzj2011.0146

 doi:10.2136/vzj2011.0146

Convergent Flow in Unsaturated Fractured Chalk

Dawn. M. Keim[1*], L. Jared. West[1], Noelle. E. Odling[1]

Abstract

The Cretaceous Chalk in Northern Europe and other similar fractured rock aquifers frequently have very thick unsaturated (vadose) zones which control both their hydraulic response to rainfall and the extent to which pollutants are delayed or attenuated before reaching groundwater. Understanding their hydraulic responses is a pre-requisite for prediction of future trends in groundwater recharge and quality. Accurate characterization of these responses remain elusive because of difficulties in both obtaining in-situ measurements and in devising appropriate conceptual models of flow processes in unsaturated fractured rock. In this study we addressed both issues by simultaneously monitoring soil water dynamics through continuously logged matric potential and moisture content and measuring discharge into a subsurface tunnel at up to 45 m depth within the unsaturated zone of Cretaceous Chalk in Northern England. Winter drainage fluxes from the base of the soil zone were estimated using the HYDRUS code for one-dimensional variably saturated media. Comparison of soil zone drainage representing the hydraulic input into the Chalk unsaturated zone with tunnel discharge provides insights into the flow dynamics of the unsaturated zone. The relative magnitudes of the soil drainage and deeper unsaturated zone discharge show that flow pathways converge resulting in increased flow focussing with depth in the unsaturated zone. The observed short lag times between the soil surface and the inflow sites in the subsurface tunnel suggest that contaminants from the surface could rapidly reach the water table through thick unsaturated zones within the Chalk.

Dawn. M. Keim[*], L. Jared. West, Noelle. E. Odling, Earth Surface Science Institute, School of Earth and Environment, University of Leeds, Leeds, West Yorkshire, LS2 9JT, UK

1. Introduction

The unsaturated (vadose) zone plays a crucial role in the hydrological cycle in that it controls the movement and flow of water and solutes from the ground surface. It provides a buffer in which contaminants applied at the surface may be delayed and attenuated before reaching the water table. It also plays an important role in reducing groundwater flooding by temporally spreading the impact of storm recharge events on the water table response. The extent of this buffering effect depends on the characteristics of the unsaturated zone but it is particularly difficult to measure in dual porosity fractured lithologies like the Cretaceous Chalk of the UK and Europe where flow and solutes can be rapidly moved through the system via preferential fracture pathways or more slowly through the porous matrix. The quantification of recharge and characterisation of flow and transport in the Chalk unsaturated zone is not an easy task and despite several decades of study considerable uncertainty remains regarding the dominant flow regime (e.g. Smith, 1970; Headworth, 1972; Wellings, 1984; Geake and Foster, 1989; Price et al., 1993; Ireson et al., 2006; Lee et al., 2006; Ireson and Butler, 2011).

Uncertainty regarding the response of the deeper unsaturated zone arises partly due to difficulties in quantifying drainage water leaving the base of the soil zone. The soil buffers and attenuates precipitation events, dependent on the soil moisture content versus depth profile at the time of a given rainfall event. Establishing the water release characteristics allows assessment of the movement of water in the soil zone and can be achieved by monitoring moisture content and soil tension, and through the application of numerical modelling. However, monitoring depth is generally limited to the top several meters of the unsaturated zone due to difficulties related to device installation and maintenance. A few studies have attempted deeper moisture content monitoring in matrix flow systems; for example West and Truss (2006) installed specialist borehole packer-based instrumentation to 20 m depth in the unsaturated zone of the Sherwood Sandstone in Northern England. However, with fractured formations such as the Cretaceous Chalk it is rarely possible to obtain meaningful in-situ measurements deep within the unsaturated zone via boreholes because flow becomes concentrated in fractures or conduits which may or may not be intersected by these boreholes. Hence, most previous studies have focussed on inferring the nature of unsaturated zone flow processes from solute profiling in extracted cores, tracer testing or numerical simulations of water table response to rainfall.

Prior to the 1970s, it was widely accepted that flow through the Chalk unsaturated zone was predominately via the fracture network, which was largely supported by observations of fast water table response to rainfall (Headworth, 1972). However, fast water table response is also compatible with piston displacement (via pressure diffusion) of pore fluid via the Chalk matrix (Price et al., 1993) and subsequent studies led workers to believe that flow through the Chalk unsaturated zone was in fact predominately facilitated via the Chalks intergranular matrix. For example, Smith et al., (1970) reported tritium profiles from cores following thermonuclear testing that produced high tritium concentrations in rainfall during 1963-1964 and 1958-1959 respectively. The position of two peaks corresponding to these events was used to calculate a mean downward solute transport rate of less than 0.1 $mmhr^{-1}$ (2.4×10^{-3} md^{-1}) which was interpreted to indicate flow predominantly through the matrix. Wellings (1984) carried out artificial deuterium oxide tracer testing at a site in Hampshire (Southern England) and also reported a slow downward transport rate of 0.1 $mmhr^{-1}$ which was attributed to matrix flow. However, in a re-interpretation of these data-sets, Geake and Foster (1989) and Barker and Foster (1981) proposed that the apparent slow downward migration of these solute peaks was in fact caused by a combination of relatively rapid downward flow via the fracture network and lateral diffusion of solutes into the matrix blocks. In other words solute profiling studies are not diagnostic as they could indicate either flow mechanism.

Since the study of Headworth (1972) only a handful of studies have been undertaken on the UK Chalk which focus on the correlation between rainfall and in water level rise. Ireson et al., (2006) analysed cumulative water table rise in comparison to effective rainfall over the 2003/2004 hydrological year at a site in Southern England. They reported a peak lag time between effective rainfall and water table rise indicating a downward pressure pulse propagation rate of 125 $mmhr^{-1}$ (3 md^{-1}). Although it was acknowledged that this rate of percolation could indicate preferential flow in fractures, it is also compatible with pressure diffusion through the matrix (Barker, 1993). However, in a subsequent study Ireson and Butler (2011) argued that preferential flow through fractures was the dominant mechanism following an observation of very rapid water table response indicating downwards pressure pulse propagation at 1700 $mmhr^{-1}$ (40 md^{-1}). Lee et al., (2006) conducted a cross-correlation study of time series of rainfall and borehole water level at six sites in Southern England to investigate seasonal variations in water table rise response times. A one-dimensional diffusive equation was used to test if estimated response times could be attributed to pressure diffusion via the matrix; although some of the slower responses could be explained in this way more rapid responses were interpreted to indicate fracture flow. They also found that lag time was highly dependent on the season and related to the saturation level of the

 doi:10.2136/vzj2011.0146

unsaturated zone at the time of a recharge event. In order to understand such seasonal behaviour, numerical models have been applied which simulate both matrix and fracture flow in the Chalk unsaturated zone (e.g. Mathias et al., 2006; Ireson et al., 2009; Ireson and Butler, 2011). However, these are essentially one-dimensional, i.e. they all assume laterally uniform, vertical downwards flow, and do not attempt to model the influence of highly conductive fracture pathways. We believe that a much improved conceptual understanding of the nature and dimensionality of flow in unsaturated Chalk is required in order to be able to accurately predict water table response and solute migration rates through the unsaturated zone.

In order to develop such an understanding, here we report a fusion of field monitoring and modelling techniques to characterize flow processes in unsaturated chalk. Previous work at the site of the study reported here is described in Allshorn et al., (2007) who carried out qualitative (Photine-CU) and quantitative (Rhodamine and Fluorescein) tracer test experiments in the unsaturated zone of the Chalk. The tracers were injected into the top of the unsaturated zone and recovered in a subsurface tunnel. The observed tracer travel times provided evidence of fast solute transport with velocities up to 792 mmhr^{-1} (19 md^{-1}). Here we present a more comprehensive study of the unsaturated zone at this site, using high temporal resolution monitoring of soil zone drainage and tunnel discharge. We simultaneously monitored soil water dynamics, through the measurement of continuously logged matric potential and moisture content, and tunnel discharge at depths of up to 45 m below the ground surface. Drainage fluxes from the soil zone were estimated from soil monitoring data using the HYDRUS code (Simunek et al., 2008) for one-dimensional variably saturated media and the timing of the individual soil zone drainage events are compared with corresponding discharge responses in the tunnel.

 doi:10.2136/vzj2011.0146

Extensive geological logging of exposures within the tunnel was carried out in order to identify the physical characteristics of the deep unsaturated zone. The results are used to inform a conceptual model of the Chalk unsaturated zone, which may form the basis of future numerical modelling of its hydraulic response.

2. Study site

Located on agricultural land in the Yorkshire Wolds of Northern England, the study site is situated approximately 15 km south-east of Market Weighton (Figure 1a). The Wolds represent the unconfined NW section of the Northern Province Chalk, and consist of a network of dry valleys. Annual rainfall on the Wolds is ~750 mm and there is little surface drainage as topography rarely intersects the water table (Gale and Rutter, 2006).

Like most Chalk aquifers in the UK, the soil at this site is relatively thin (~0.3 m) and permeable. Porosity ranges between 34 and 49% at depths down to 0.8 m (Table 1). The National Soil Resources Institute (2009) classifies the soil type at this site as a silty clay loam within the Andover soil series which correlates to the US soil sub-group Lithic Haprendolls, sub-order Rendolls (U.S. Department of Agriculture Keys to Soil Taxonomy 2010). Figure 2 shows the soil profile at the installation pit site, which can be divided in to four horizons; 0 – 0.3 m (silty clay loam), 0.3 – 0.6 m (silty clay loam and highly weathered Chalk), 0.6 – 1 m (highly weathered Chalk), and 1 – 1.5 m (moderately weathered Chalk). A thick (~0.1 m) discontinuous flint band is present at ~0.7 m depth.

 doi:10.2136/vzj2011.0146

This thin soil and weathered Chalk layer (0 – 1.5 m) is underlain by a further 2 - 3 m of slightly weathered Chalk which is in turn underlain by up to 95 m of unsaturated unweathered Chalk. A 2 km long subsurface tunnel deep within this unsaturated zone provides access to a 1250 m long panel (~2 m in height) of exposed Chalk (Figure 1b). The base of the panel is situated at approximately 75 mASL (meters above sea level) and, as the topographic elevation of the ground surface is 90 – 130 mASL, its depth below the ground surface ranges between 30 and 45 m. The water table is located at approximately ~35 mASL, which places much of the exposed Chalk panel in the middle of this thick unsaturated zone.

The Chalk gently dips 1 - 2 degrees to the east at the study site. Previous geological studies determined that the site is stratigraphically within the Burnham Chalk Formation (Allshorn, 2008) which was deposited during the Late Cretaceous. A Chalk sample from the subsurface tunnel exposure (~45 m overburden) gave a porosity (determined using a helium pycnometer) of 19.8% and a hydraulic conductivity of 9.6×10^{-3} mmhr^{-1} (2.3×10^{-4} md^{-1}). The Chalk sequence exposed in the tunnel is comprised of finely bedded laminate chalk (beds 0.02 – 0.2 m thick) with massively bedded chalk (beds 0.4 – 0.8 m thick) occurring towards the eastern end of the tunnel. Marl horizons, nodular and discontinuous flint layers are present throughout. Marl flasering with thin (<0.002 m) intertwining marls also occurs. Of particular interest is the presence of rare paramoudra which are large cylindrical flint nodules in-filled with chalk and up to 1 m in height (Brenchley, 2006).

The fracture network was characterised through systematic measurement of the orientation and aperture of all non-strata bound fractures that cut the entire 2 m exposed panel (intersecting both the floor and ceiling boundary) of the north facing wall of the tunnel exposure. In total, 128 fractures were logged giving an average spacing of 8.5 m with variable apertures ranging from <1 mm to several centimetres. An equal area stereographic projection of fractures plotted as poles to planes is shown in Figure 3. This shows that there are two distinct sets of fracture poles indicating a conjugate fracture set. The mean principal orientation of the western pole series is 61/097 (dip/dip direction) while the mean principal orientation of the eastern set is 62/244.

Sparse pipe-like features of the order of centimetres in diameter are present along some major fracture planes and fracture intersections. The largest of these features is choked with clay rich sediments of probable glacial origin, suggesting that it was formed prior to the last glaciation (some 11000 years ago). Other smaller open voids of 1 - 2 cm diameter also occur along fractures. Where these channel ways are water bearing, they show strong inflow into the tunnel. The presence of such features results in an inhomogeneous distribution of flow across the length of the tunnel ceiling and walls.

3. Field Monitoring

In this study, we monitored soil water dynamics through the simultaneous measurement of continuously logged matric potential and moisture content along with rainfall, and subsurface tunnel inflows at depths of up to 45 m below the ground surface. Monitoring at 15 min intervals began at the start of the 2009/2010 hydrological year (1-Oct 2009). Data from the time period 1-Oct 2009 to 30-Sept 2010 are reported here. Soil sampling was also carried out to determine soil porosity and is described below.

 doi:10.2136/vzj2011.0146

3.1. Soil Sampling

The study incorporated three soil sampling sites, F1, F2 and F3, located above the subsurface tunnel at chainages of ~725, ~1025, ~1325 m from the tunnel's western portal respectively (Figure 1b). The sampling sites were specifically selected with the aim of measuring the variability in soil properties across the length of the tunnel and as such each was under a different land management regime throughout the study period with F1 cropped with field peas, F2, grazed permanent grassland, and F3 cropped with winter wheat.

Shallow cores of 1 m length (0.45 m diameter) were extracted from the ground surface at each of the sample sites using a manual percussion drill (Cobra, Atlas-Copco UK Holdings Ltd.) and foil lined window-less sampler. Following standard field soil sampling methodologies (Rowell, 1994), samples obtained from cores were processed and analysed for moisture content and dry bulk density (DBD). Porosity was then estimated by assuming a soil particle density of 2650 kg/m^3 for soil samples, and 2710 kg/m^3, the density of calcium carbonate, for Chalk samples (Rowell, 1994).

3.2. Experimental Soil Plot

A 1.5 x 1.5 x 1.5 m soil monitoring pit was excavated ~40 m above the subsurface tunnel and was instrumented in September 2009 (see Figure 1b). The monitoring pit, situated at the same location as core extraction site F3, is located approximately 1325 m from the western end of the tunnel and approximately 200 m west of drip collection site D3. As depicted in Figure 4, the monitoring pit was equipped with a tipping bucket rain gauge (Young Ltd, Model 52203) and logging soil moisture content and tension monitoring devices.

The tensiometers (UMS Umweltanalytische Mess-Systeme GmbH, Model TS1s) were installed horizontally along the southern wall of the pit at depths of 0.5, 1, 1.5 and 2 m. The moisture sensors (IMKO Micro- modultechnik GmbH, Model 64/32 Trime-Pico), which are based on TDR (Time-Domain-Reflectometry) technology, were installed horizontally along the northern wall of the pit at depths of 0.4, 0.6 and 0.8 m. The rain gauge and devices were wired to a central distribution module connected to a logger (IMKO Micro- modultechnik GmbH, Globelog Logger). The logger was equipped with a GSM (Global System for Mobile) antenna, which enabled remote telemetry data transmissions. After installation, the pit was backfilled such that it could be sown (with winter wheat) along with the surrounding field.

3.3. Subsurface Installations

The subsurface tunnel was equipped with three drip collection units labelled D1, D2 and D3, located at depths of 45 m (D1 and D2) and 30 m (D3) beneath the ground surface (Figure 1b). As shown in Figure 5, each unit consisted of a 2 x 2 m collection area (made of polyethylene plastic) which channelled drip water through a funnel situated above a tipping bucket rain gauge (EM Ltd. ARG100-DT2, developed by CEH Wallingford). The rain gauges were equipped with automatic loggers (EM Ltd. DT2-R) that logged bucket tips, each tip equivalent to 0.002 litres.

 doi:10.2136/vzj2011.0146

Discharge volume per hour for each drip collection unit was then converted into equivalent average discharge rate ($mmhr^{-1}$) over the 4 m^2 collection area.

The collection units, D1, D2 and D3, were located at 530 m, 725 m, and at 1540 m from the western portal respectively (Figure 1b), and each was located at a strong inflow point. There is an inhomogeneous distribution of flow into the tunnel and not all sections of the tunnel ceiling discharge continuously throughout the year. Therefore care was taken to ensure drip collection sites monitored points of high discharge. The atmospheric relative humidity in the tunnel during winter months is 96% or greater (Allshorn, 2008) and therefore evaporation is considered negligible and measured discharge rates accurately represent tunnel ceiling inflow rates.

4. Soil Drainage Flux Modelling Methodology

Hourly drainage fluxes during part of the 2009/2010 winter recharge season (1-December 2009 to 15-March 2010, 2520 hours) from 1 m depth were estimated by simulating water flow at the study soil monitoring plot using the HYDRUS code (Simunek et al., 2008) for one-dimensional variably saturated media. The modelled period represents the bulk of the winter recharge season, slightly truncated for modelling purposes, to avoid issues associated with strongly hysteretic soil moisture content versus matric potential behaviour during the seasonal wetting and drying phases. HYDRUS numerically solves water flow in unsaturated media using the Richards equation:

 doi:10.2136/vzj2011.0146

$$\frac{\partial \theta}{\partial t} = \frac{\partial}{\partial z}\left[K(h)\left(\frac{\partial h}{\partial z} + 1\right)\right] \quad . \qquad (1)$$

where, h is the soil water pressure head [mm], θ is the volumetric moisture content [-], t is time [hr], z is the vertical spatial coordinate [mm] and $K(h)$ is the hydraulic conductivity as a function of pressure head [mmhr^{-1}]. Soil hydraulic properties were modelled using the Mualem - van Genuchten hydraulic model (van Genuchten, 1980; Mualem, 1976) given by equations (2) and (3) below:

$$\theta(h) = \begin{cases} \theta_r + \dfrac{\theta_s - \theta_r}{[1 + |ah|^n]^m} & h < 0 \\ \theta_s & h \geq 0 \end{cases} \quad . \qquad (2)$$

where θ_s is saturated moisture content [-]; θ_r is residual moisture content [-]; K_s is saturated hydraulic conductivity [mmhr^{-1}]; α is an air entry parameter [mm]; n is a pore size distribution parameter [-]; and l is a pore connectivity parameter [-] fixed at 0.5 (Mualem, 1976), and

$$K(h) = K_s S_e^l [1 - (1 - S_e^{1/m})^m]^2 \quad . \qquad (3)$$

where S_e is effective saturation given by:

$$S_e = \frac{\theta(h) - \theta_r}{\theta_s - \theta_r} \quad . \qquad (4)$$

 doi:10.2136/vzj2011.0146

and

$$m = 1 - 1/n, \qquad n > 1 \tag{5}$$

The soil hydraulic parameters θ_r, θ_s, α, n and K_s in equations (2) – (5) are independent parameters assigned to each layer of the model.

Three layers have been defined in our model, each corresponding to a different horizon in the top 1 m of the soil plot profile (Figure 2). The top layer (silty clay loam) spans from 0 – 0.3 m depth, while the second (silty clay loam and highly weathered Chalk) and third (highly weathered Chalk) layers span from 0.3 – 0.6 m and 0.6 – 1 m depth, respectively. The modelled profile (1 m) was descretized using a uniform finite element cell length of 0.01 m (101 nodes in total). An atmospheric boundary condition (dependant on rainfall, infiltration and evaporation) was used for the upper boundary condition and free drainage was used for the lower boundary condition. The initial conditions were set by assigning observed pressure head values at 0.5 and 1 m depth (at 01:00 hr, 1-Dec 2009) to the corresponding nodes within the model, from which an initial linear distribution of pressure head with depth was imposed.

Rainfall data for the model input were obtained from the rain gauge at the experimental site, and where necessary, missing data (e.g. due to the rain gauge being disconnected for crop spraying) was provided from the UK Meteorological Office records from the nearest weather station located in Leconfield some 15 km away. Evapotranspiration, *ETp*, was estimated in HYDRUS using the Hargreaves equation (Jensen et al., 1997) and mean daily maximum and minimum air temperatures provided by the Meteorological Office (Leconfield weather station). The Hargreaves equation is expressed as:

$$ETp = 0.0023 R_a (T_m + 17.8)\sqrt{TR} \quad . \qquad (6)$$

where R_a is extraterrestrial radiation [J m^{-2} s^{-1}], T_m is mean daily air temperature (based on mean daily minimum and maximums) [°C] and TR is temperature range between minimum and maximum values [°C]. Extraterrestrial radiation, R_a, is computed within HYDRUS from the latitude and altitude of the study site. Plant water uptake will have been close to nil over the period modelled (1-Dec 2009 to 15-Mar 2010) due to the low temperatures and early crop stage (crops will have been mostly dormant) and therefore no crop cover was assumed and thus the ETp estimate from Equation 6 essentially represents evaporation.

The five independent soil hydraulic parameters (θ_r, θ_s, α, n and K_s) were optimized within HYDRUS using an inverse technique based on the Levenberg-Marquardt nonlinear minimization method (Simunek et al., 2008) to estimate model parameters by fitting to a subset of the measured moisture content and matric potential data obtained from the logged soil plot monitoring site. Measured moisture content data from the probes at 0.4 and 0.6 m depth and matric potential from the probes at 0.5 m and 1 m depth were used. The moisture content probe at 0.8 m depth was omitted from the modelling process because of the lower than expected moisture content readings due to the presence of an overlying flint layer with low hydraulic conductivity.

 doi:10.2136/vzj2011.0146

The objective function within the inversion solution contained 5040 data points of equal weight which comprise bi-hourly measurements from the four measurement probes selected for the inversion process (i.e. 1260 data points per measurement probe). Weighting of inversion data was by standard deviation and the maximum number of iterations was limited to 10. Although HYDRUS allows simultaneous optimization of up to 15 parameters, we performed simultaneous optimization for a maximum of six parameters to minimise issues with potential non-uniqueness of the solution. Minimum and maximum limits were set for parameters, θ_r, θ_s and K_s, while no limits were imposed on the empirical shape parameters α and n. The parameter range for θ_r was taken from the Carsel and Parrish (1988) soil catalogue integrated in HYDRUS for sand (5% Vol.) and silty clay loam (9% Vol.). The minimum parameter value limit for θ_s is based on the measured porosity, 20%, of a consolidated chalk sample from the site and the upper limit was set at 49% which represents the highest measured porosity value at core site F3 (Table 1). The minimum value for K_s was taken from the Carsel and Parrish (1988) soil catalogue for silty clay loam (0.7 mmhr^{-1} or 1.7 x 10^{-2} md^{-1}) and the maximum value was set at 10,000 mmhr^{-1} (240 md^{-1}) which is thought to be an acceptable value for weathered, high flow zones in the Chalk unsaturated zone (Gale and Rutter, 2006; Allen et al, 1997; Foster and Milton, 1974).

Optimization was performed sequentially for the parameters in each layer (i.e. θ_r, layer 1; θ_s, layer 1; α, layer 1...) and repeated for each layer in order of depth. For each layer, a final optimization run was performed to check on the validity of the parameter set for that layer. Finally, optimization using selected parameters for all model layers (i.e. θ_r and θ_s, layer 1 – 3; α and n, layer 1 – 3; K_s, layer 1 -3) was run to check on the validity of the complete final parameter set. This procedure was devised because problems were encountered in obtaining an automatic fit for all parameters simultaneously from initial estimates. It was found that the automatic fitting facility in HYDRUS worked only when initial values were relatively close to the final solution. To check that a global minimum has been reached, runs were made using variations on the initial input parameters to ensure that the model consistently converges on the final data set determined above.

5. Results

5.1. Field Monitoring

Soil Porosity

Porosity values obtained through shallow core sampling are generally somewhat higher and more variable within the top 0.4 m of the soil profile (ranging from 34 to 49%) and decrease in the deeper (highly weathered chalk) horizons between 0.6 and 0.8 m (ranging from 35 to 41%), see Table 1. Soil porosity values at F1 and F3 are remarkably similar (39 to 49%), while porosity is generally lower (34 to 40%) at F2 which is likely due to the well structured and rooted soil (typical of permanent grassland) and compaction from animal grazing. Gravimetrically measured moisture content values at site F3 are consistent with those measured using the TDR instrumentation (see *Soil Moisture Content* sub-section below) installed at the same location (Table 1), except for the TDR probe at 0.6 m depth which was close to a discontinuous flint layer. Based on these sampling results and inspection of surface soils along the line of the tunnel

 doi:10.2136/vzj2011.0146

soil properties seen at sites F1 – F3 are likely to be representative of the soils above the tunnel elsewhere.

Soil Moisture Content

Automatically logged TDR volumetric soil moisture content measured over the 2009/2010 hydrological year is presented in Figure 6b and ranges between 13 and 33% Vol. These extremes were both recorded from the probe installed at 0.6 m depth. Readings from this layer showed the greatest level of moisture content variability. This is possibly due to the presence of an underlying flint layer that may have caused water to pond throughout the recharge season but allowed drainage in the summer months. Soil moisture content was also quite variable at the shallowest probe depth of 0.4 m, ranging between 15 and 29% Vol. Moisture content variability is attenuated with depth and is least variable (20 - 29% Vol.) within the highly weathered Chalk layer at the probe depth of 0.8 m.

For the most part, moisture content within the profile remained below 25 to 26% Vol. throughout the warmer summer months during crop growth from mid-April to end-September 2010 when evapotranspiration (*ETp*) is likely to exceed rainfall. Despite the occurrence of several rainfall events during October 2009, moisture content remained relatively low due to the moisture deficit in the profile built up over the previous summer months. Higher moisture contents were observed throughout the winter months (November 2009 – April 2010) when rainfall largely exceeded *ETp*. During this period, baseline moisture content values remained fairly constant at ~27% Vol. at 0.4 and 0.8 m depth and ~30.5% Vol. at 0.6 m depth. Moisture content fluctuations

doi:10.2136/vzj2011.0146

at the probe depth of 0.8 m are less than expected which may be explained by the presence of the overlying flint layer at 0.7 m depth which reduces the impacts of precipitation and evaporation. Several sharp peaks in moisture content are observed (on 15/12/09, 26/12/09, 15/01/10, 20/01/10, 05/02/10, 15/02/10 and 25/02/10) each of which is followed by a slow decrease. The sharp peaks represent soil moisture content values approaching saturation as a result of large rainfall events and the slow decreases represent soil drainage.

Matric Potential

Matric potential readings over the 2009/2010 hydrological year are shown in Figure 6c. The matric potential rose sharply during the wetting phase (from below the probe measurement limit of -8.5m, to -0.5 m H_2O), which took place from the end of October to mid-November 2009, a process which spanned approximately two weeks. Measurements prior to ~Nov-1 2009 which are below the probe measurement limit of -8.5 mH_2O are therefore regarded as inaccurate. Following 1-Nov 2009, wetting was detected first by the top probe (0.5 m depth) and then progressively with increasing depth. Matric potentials remained greater than -0.5 m H_2O throughout the profile from mid-November 2009 to mid-April 2010 indicating that drainage was taking place throughout this period (the winter recharge season).

Reduction in matrix potential caused by drying of the soil started to take place around mid-April 2010, first occurring in the top of the soil zone and gradually progressing through the profile to the deepest probe at 2 m depth. Matric potentials throughout the profile dropped sharply following the initial drying and neared the measurement limit of -8.5 m H_2O towards mid-May

2010 when the devices appear to have cavitated due to lack of sufficient water to re-fill. Therefore measurements beyond mid-May 2010 are regarded as inaccurate.

Subsurface Discharge

Discharge rates recorded at the drip collection sites (D1, D2 and D3) in the subsurface tunnel varied in both magnitude and timing over the monitoring year (as shown in Figure 6d-f). Discharge rates vastly exceeded the measured hydraulic conductivity, K_s, of the Chalk matrix (9.6×10^{-3} mmhr^{-1}) and varied from 0.32 to 3.17 (mean 1.00), 0.02 to 3.03 (mean 0.28) and zero to 2.75 (mean 0.46) mmhr^{-1} at D1, D2 and D3, respectively. The mean discharge rates at each drip site recorded over the high discharge period (15-Nov 2009 to 15-May 2010) were 1.42, 0.47 and 0.90 mmhr^{-1} at D1, D2 and D3 while mean discharge rates over the drier summer months (15-May to 30-Sept 2010) were 0.68, 0.10 and 0.01 mmhr^{-1}.

Three major discharge events are observed to have taken place over the high discharge period. These events are most distinct at D2 where maximum peak discharge rates of 2.00, 1.90 and 3.03 mmhr^{-1} were observed on 7-Dec 2009, 23-Jan 2010 and 27-Feb 2010 respectively. These events were less distinct at the other sites where several smaller events were also observed. The gaps in discharge rate data at D1 are due to repeated problems that were encountered with the data logger.

The characteristic shape of the major peak discharge events is similar to the shape of the drainage curves from the soil zone where soil moisture content rapidly rises and then slowly drains back. The sharp peaks in discharge are followed by a slow decay; it generally takes ~24 hr for an event to peak and several days for the discharge rate to return to baseline level or pre-peak rate.

5.2. Modelled Soil Hydraulic Responses and Drainage Flux

Figure 7b - d presents simulated moisture content and matric potential data plotted with observed data for each of the respective measurement depths within the top 1 m of the soil plot profile (moisture content at 0.4 and 0.6 m, and matric potential at 0.5 and 1 m depth) for the period of 1-Dec 2009 to 15-March 2010. The model generally predicts moisture content and matric potential values that are in good agreement with the observed data, although fails to match the magnitude some of the extreme minima and maxima. The final model parameter sets applied to the model period 1-December 2009 to15-March 2010 (2520 hours) are presented in Table 2. A final square of the correlation coefficient, r^2, of 0.96 for the fit between model estimates of moisture content and matric potential and observed moisture content and matric potential was obtained.

The HYDRUS simulated soil drainage from 1 m depth for the period of 1-Dec 2009 to 15-March 2010 is presented in Figure 7e. The soil drainage output flux at 1 m depth is remarkably smooth in comparison to observed rainfall at the ground surface (Figure 7a) which is a good indication of soil zone buffering effects. Three distinct soil drainage peaks of substantial magnitude (labelled P1, P2 and P3 in Figure 7e) are estimated to have taken place at maximum rates of 2.65, 2.10 and 2.23 mmhr^{-1} on 06-Dec 2009, 22-Jan and 26-Feb 2010, respectively. The duration of these

 doi:10.2136/vzj2011.0146

drainage events (based on the time intervals from peak to half peak height) was 12, 28 and 32 hours with cumulative drainage of 11.9, 14.72 and 21.17 mm for P1, P2 and P3, respectively.

Each of these major drainage events followed rainfall events greater than 2 $mmhr^{-1}$. However not all rainfall events of this magnitude resulted in major drainage events. This is related to the soil moisture content through the profile at the time of a given rainfall event. When the moisture content throughout the profile was near saturation at the time of a major rainfall input, rapid drainage ensued whereas when the moisture content throughout the profile was significantly below saturation, a slower and less intense drainage ensued. The latter is clearly the case for the smaller drainage events predicted to have taken place on 02, 15, 27-Dec 2009, 17-Jan 2010 and 17-Feb 2010 (Figure 7e), which all followed substantial rainfall input (>1.5 $mmhr^{-1}$), but never exceeded drainage rates of 0.32 $mmhr^{-1}$.

In Figure 8 we present the modelled SMC curve for layer 2 (0.3 to 0.6 m depth) alongside data from the tensiometer at 0.4m depth and the moisture probe at 0.5m depth, collected during the model period of 1-Dec 2009 to 15-Mar 2010. Data corresponding to the three soil drainage peak events P1, P2 and P3, identified in Figure 7e, are highlighted. Data describe three distinct trends; i) a relatively horizontal band, falling below the modelled SMC curve, corresponding to data from December 2009, where the measured moisture content does not vary much with matric potential (it mainly falls between 26.5 and 27.5 % Vol.), ii) a band corresponding to the remainder of the modelling period, where there is a strong relationship between moisture content and matric potential, which is described well by the modelled SMC curve and iii) a series of 'wetting loops' which plot above the main data cloud and the SMC curve, i.e. relatively high moisture contents for a given matric potential (the temporal progression of these loops is indicated using arrows). Two of these wetting loops correspond to the peak drainage events P2 and P3; two smaller loops are visible corresponding to more minor wetting events which took place on 16 and 24- Feb 2010. These wetting loops are only a few hours in duration, and are likely to represent an artefact of the instrumentation; the rise in matric potential on rapid wetting takes a few hours to penetrate the porous ceramic tips of the tensiometers, so their response lags behind that of the moisture probes. The lack of variation in moisture content seen during the first month of the modelling period (Dec 2009), despite the wide fluctuations in matric potential, suggests the development of heterogeneous flow pathways in the upper 0.5m – i.e. the tensiometer intersected a wetting pathway, whereas the moisture probe which is 1.5 m away laterally, did not. Later in the modelling period (Jan 2010 onwards) both probes respond together, which indicates that more homogeneous flow conditions had developed. Within this main band representing Jan – Mar 2010, the vertical spread in the data of around 0.5 % Vol. moisture content reflects hysteresis. This relatively small degree of hysteresis is comparable to those seen at similar depths in the Chalk presented in Ireson et al., (2006), and allows the behaviour during this period to be adequately represented by a single SMC curve.

5.3. Comparison of Estimated Soil Drainage and Subsurface Discharge

Here we compared the HYDRUS simulated drainage flux from 1 m depth to the subsurface tunnel discharge rates at D1, D2 and D3 over the modelled winter recharge season (1-Dec 2009 to 15-Mar 2010). Both the magnitude of the cumulative discharge and the timing and shape of peak events (P1, P2 and P3) are examined and differences in responses are linked to factors such as unsaturated thickness and fracture spacing.

Geological Features

The total number of logged fractures (non-stratabound fractures which extend beyond the height of the exposed tunnel panel) within 100 m on either side of each drip collection site was used to calculate the mean fracture spacing around each site. Average fracture spacing is least near D1 (4.6 m) followed by D3 (7.1 m) while D2 has the greatest fracture spacing (9.2 m). Fracture spacing at D2 and D3 are close to the average value and that at D1 is around half the average spacing for the entire tunnel (8.5 m). Stratigraphic logging of visible strata exposed in the tunnel walls was used to identify the main sedimentary features present in 10 m sections of chalk above each drip collector. The main features present above D1 include six continuous flint bands, two marl bands and two layers showing marl flaser structure while three continuous flint bands and eight marl bands are present above D2. It was not possible to log the features above D3 due to lack of exposure of the relevant stratigraphy. As previously reported the total unsaturated chalk thickness above D1 and D2 is 45 m, and 30 m above D3 (see Figure 1b).

Hydraulic Responses

Simulated cumulative drainage from the soil zone (mm) and observed cumulative subsurface discharge (mm) values reported over the modelled recharge season (1-Dec 2009 to 15-March 2010) are presented in Table 3. The cumulative discharge at D1 is 28 times greater than the estimated cumulative drainage from the soil zone while that at D2 is 10 times and that at D3 is 20 times greater. The fact that tunnel discharges are much greater than the soil drainage estimate indicates a large degree of flow focussing, i.e. convergent flow in the unsaturated zone of the Chalk. Differences between the cumulative discharges at the different drip sites imply variations in surface catchment area that feed each drip collector (see Table 3).

To compare the hydraulic responses of drip collectors D1, D2 and D3 in the tunnel to the individual peak soil drainage events P1, P2 and P3, details of the data presented in Figure 7 at the times of the soil drainage events is re-plotted in Figure 9 and a summary of key statistics relating to each response is presented in Table 4. The time lag between the peak event in the soil drainage signal and in the tunnel was the least for D3 (between 11 and 18 hours) where the thickness of unsaturated chalk is least (30m). Larger time lags of between 18 and 27 hours at D2 and between 99 and 125 hours at D1 occur where the unsaturated chalk thickness is greatest at 45m (Figure 9 and Table 4).

In all cases peak breadths observed at the drip sites are greater than those estimated for soil drainage at 1 m depth. The mean duration of a peak discharge event (characterised as time from peak discharge rate to half that rate) was the longest at D1 (376 hr) followed by D3 (125 hr) and the shortest at D2 (50 hr) while all peak soil drainage event durations were between 12 and 32 hr. The ratios of peak discharge event duration at each subsurface drip site to that of the corresponding soil drainage peak events are shown in Table 4. The greatest ratio is observed at D1 where a peak discharge event lasted 188 times longer than the peak soil drainage event. At

D3 peak discharge events lasted an average of 48 times longer and D2 showed the smallest ratio at an average of 20 times longer than the corresponding soil drainage event.

A complete analysis of the hydraulic response at D1 to soil drainage events was not possible due to gaps in the data caused by logger malfunction. However, the available data suggests that behaviour at this site is significantly different to the others. As shown in Figure 9 and Table 4, there is a much longer delay (lag) in the hydraulic response at D1 where the cumulative discharge and peak discharge event duration far exceed those at the other two sites. This may be related to the relatively close fracture spacing observed at this site compared to other sites.

6. Discussion

In this study we have developed a quantitative method for assessing flow in the Chalk unsaturated zone through a fusion of intensive field monitoring and numerical modelling of the soil zone. Comparison of hydraulic responses observed at tunnel drip monitoring sites deep within the Chalk unsaturated zone with the soil zone drainage response is used to develop a better understanding of lithological controls on the nature of flow processes in a thick unsaturated zone within the fractured Chalk.

The estimated rates of soil drainage entering the top of the Chalk unsaturated zone and the observed discharge rates in the deep subsurface at drip monitoring sites vastly exceed the measured K_s of the Chalk matrix over the entire recharge season and hence observed discharge at this site is inferred to be largely facilitated via the fracture network. Further, lag times between peak soil drainage events (at 1 m depth) and peak discharge events in the tunnel at 30 to 45 m depth (Table 4) varied between 11 and 125 hours (~0.5 – 5 days). Following Ireson et al., (2006) the characteristic time equation for pressure diffusion through the Chalk matrix (Barker, 1993) is:

$$t_{cb} = b^2 S_s / K_s \quad . \tag{7}$$

where t_{cb} is characteristic time for pressure diffusion through a matrix block [d^{-1}], b is the matrix block width [m], and S_s is the specific storage [m^{-1}]. In our case b represents the thickness of the unsaturated zone above a given tunnel discharge monitoring site (30 or 45 m), S_s is assumed to be the minimum reported in Allen et al., (1997) for the Upper Chalk in Northern England (0.66 x 10^{-5} m^{-1}) and K_s taken as the measured value from a core sample at the site (2.3 x 10^{-4} md^{-1}). These input parameters yield a characteristic time of 25 and 58 days through 30 and 45 m of unsaturated chalk, respectively. Such values are much greater than the observed lag times between peak soil drainage events and the corresponding peak discharge events at the monitoring sites in the tunnel of 0.5 to 5 days. We infer from these calculated characteristic times that pressure diffusion of recharge pulses through the deep unsaturated zone resulting from peak soil drainage events could not have been transmitted via the matrix and were therefore facilitated through the fracture network. Although we cannot discount matrix flow altogether, its relative contribution during the winter recharge period is therefore thought to be minimal. Summer discharge, when there is no input to the system from the soil zone because of a moisture deficit, is seen most strongly at drip collectors D1 and D2 (see Figure 6d and e) and is thought to represent drainage of stored water within the unsaturated zone. Discharge ceased at D3 from 12-

doi:10.2136/vzj2011.0146

June 2010 to the end of the hydrological year (30-Sept 2010), but continued at the other two sites (D1 and D2) where the thickness of unsaturated chalk is greater (Figure 6d-f). The calculated characteristic time for diffusion (25 days at D3 and 58 days at D1 and D2) suggests that discharge up to ~1-May 2010 (at D3) and ~1-June 2010 (at D1 and D2) may have originated partially from the matrix resulting from the last drainage event from the soil zone which occurred ~1-Apr 2010. Continued discharge following these dates is likely to have been largely derived from poorly connected fractures and or small apertures on fracture surfaces. The Chalk matrix itself has pore throats (typically less than 1 μm) that are far too small to allow drainage when there is no input into the system from the surface (Price et al., 1976).

The results of this study suggest that flow at depth within the unsaturated zone is focussed in a few fractures. This can be seen from the magnitude of cumulative tunnel discharge at each of the monitoring sites which vastly exceeded the estimated soil drainage at 1 m depth (Table 3). We infer from this that the cumulative discharge recovered at the tunnel monitoring sites represents surface catchment areas of between 10 m^2 and 28 m^2 (Table 3). Results of tracer tests presented by Allshorn (2008) also indicated a lateral component to unsaturated zone flow, consistent with flow convergence between the surface and the tunnel. In Allshorn's studies, tracer breakthrough was observed in the tunnel at ~38 m below and at a horizontal distance of 50 m from the point of injection at the surface. This suggests that in some cases flow may be focused from a larger catchment area than that estimated here, or alternatively, that catchment areas may have elongate rather than square shapes. These results are broadly consistent with the observed fracture dip in the tunnel exposure (mean dip of 60° with a range of dip directions). If a fracture is continuous from the tunnel to the ground surface through an unsaturated thickness of 45 m, this fracture would intersect the ground surface with a horizontal displacement of ~26 m from its starting point in the tunnel. The flow convergence observed in this study and in that of Allshorn (2008) is likely to result from flow along fractures with this dip. Flow is likely to be distributed evenly near the ground surface and become progressively focussed with depth which explains the observed highly inhomogeneous distribution of flow entering the tunnel.

Recently Ireson and Butler (2011) looked at the occurrence of rapid bypass flow in fractures within the unsaturated zone of the Southern Chalk of the Pang and Lambourn Catchments. They showed that a small number (some 3%) of rainfall events give rise to bypass flow through the fracture system which causes a significant response of the water table on time scales of less than 1 day. They also modelled the unsaturated zone response using a 1D dual continua approach which indicated that bypass flow is enhanced by relatively low matrix hydraulic conductivities of around 0.02 $mmhr^{-1}$ (5×10^{-4} md^{-1}) and low fracture porosities of around 0.1%. Where matrix hydraulic conductivity is high (>0.08 $mmhr^{-1}$), their model indicated that fracture flow is never strongly activated while for high fracture porosities (>0.1% with a fracture spacing of 0.65 m) the saturation levels within fractures never reach levels that allow rapid bypass flow. This prompted them to suggest that at depths of around 15 m only 1 in 10 fractures may be contributing to bypass flow which reduces the effective fracture porosity from 1% to 0.1%. This focussing of flow is broadly consistent with the extent of flow convergence observed in our study where the tunnel discharges exceed estimated soil drainage rates by factors of 10 to 28. Similar observations in other rock types are reported in the literature, an example being water inflow into a tunnel in unsaturated fractured Gneisses at Stripa, Sweden where around 35% of the flow is delivered by only 2% of the wall area and 70% of the wall area contributed no flow at all (Newman, 1987). Likewise, Bodvarsson et al., (2003) investigated flow focussing under unsaturated conditions in fractured tuffs using a modelling approach which suggested that flow became organized into discrete flow pathways at depth with flow rates around six times the infiltration rate, broadly consistent with our findings. Other modelling studies of fracture pathway development in soluble rocks such as limestones (Hanna and Rajaram 1998, Bloomfield et al., 2005) found that once a preferred flow pathway develops near the infiltration boundary, it is highly persistent with distance in the direction of flow and dissolution simply serves to enhance the existing structure. In their studies, this leads to the development of large pipe-like features similar to those observed in the tunnel at our site.

The results of the modelling studies described above suggest that the flow convergence observed in this study is likely to reflect the presence of dominant high aperture flow pathways that probably originate within the top 15 m of the unsaturated zone and extend to the water table. This is supported by the presence of the observed water bearing pipe-like features and open voids in the tunnel walls which suggests that dissolution has led to the development of sparse preferential flow pathways within the chalk unsaturated zone which are persistent to the level of the tunnel and were probably established many thousands of years ago. In Figure 10 we present a conceptualization of flow convergence through 50 m of the unsaturated zone in the Chalk containing conjugate fractures (with 60˚ dips) during recharge season conditions. This figure shows flow in many closely spaced fractures in the top 5 m, with a zone of flow convergence from 5 – 15 m where major fracture flow pathways are developed. Flow in these fracture pathways creates solutionally enlarged pipe-like features and voids that dominate flow, as observed in the tunnel at 30 – 45 m depth. This conceptualization illustrates how flow becomes focussed in progressively fewer fractures with increasing depth and explains other observations such as the observed horizontal displacement of water between the surface and tunnel in tracer tests (Allshorn, 2008) and our estimates of catchment area from a comparison of soil drainage rates and monitored discharge in the tunnel.

The matrix hydraulic conductivity of the Yorkshire Chalk ranges from 1-33 x 10^{-4} $mmhr^{-1}$ (Bell et al., 1999) which is significantly lower (by a minimum of an order of magnitude) than the maximum matrix hydraulic conductivity found to permit the development of focussed fracture flow in the study by Ireson and Butler (2011). This matrix hydraulic conductivity is therefore consistent with the existence of such preferential flow pathways in the Chalks at our site. Once established, such features would dominate flow during high recharge events facilitating rapid bypass flow through the unsaturated zone to the water table. The location of high discharges in the tunnel are thought likely to represent places where the tunnel has intersected such pre-existing high flow pathways rather than resulting from the presence of the tunnel itself. The observation that flow rates vary widely along the length of the tunnel and that the highest inflows are restricted to small areas of the tunnel ceiling and walls is consistent with this interpretation. Within the tunnel there is some degree of correlation between high fracture intensity and the highest inflow rates, longest lags and drainage times following peak events, illustrated particularly by the drip site D1. It is not known if the zones of high fracture intensity seen in the tunnel extend to the surface but such variations in fracture intensity would have provided the initial heterogeneities that triggered the development of a network of enhanced flow pathways resulting in flow focussing.

7. Conclusion

In this study we presented high resolution time series matric potential and moisture content data from the soil zone coupled with discharge monitoring data from deep within the Chalk unsaturated zone at a rural site in Northern England. Intensive field data collection and geological logging was carried out at our site over the 2009/2010 hydrological year. Field data were used to inform the development of a HYDRUS 1D soil water model which was used to estimate drainage fluxes from the soil zone at 1 m depth. Discharge points (drip sites) in a tunnel located between 30 and 45 m below ground surface were monitored in order to quantify the effect of the Chalk unsaturated zone on the modelled soil drainage signal and to identify flow mechanisms and their lithological controls. Identification of these flow mechanisms is important for predicting future trends in water quality and quantity in fractured Chalk aquifers. The main findings of this study can be summarised as follows:

a) As with most aquifer systems, the soil zone controls recharge to the Chalk unsaturated zone and acts as a buffer to rainfall input by absorbing and slowly releasing it either downwards as recharge or upwards as evapotranspiration. Our soil monitoring and HYDRUS modelling show how the magnitude of a given recharge event from the soil zone is dependent on the intensity of a given rainfall event, and more importantly, the soil moisture content at the time of the event. During the modelled recharge period (1-Dec 2009 to 15-Mar 2010) only rainfall events >2 mmhr^{-1} produced significant soil drainage peaks.

 doi:10.2136/vzj2011.0146

b) Winter recharge through the Chalk unsaturated zone below the soil is largely facilitated via a network of non-stratabound joints, observed in the tunnel. Estimated drainage leaving the soil zone and measured discharge entering the subsurface tunnel greatly exceed the rate at which the chalk matrix can transmit water. In addition, the rapid responses to soil drainage seen in the tunnel (between 0.5 and 5 days) suggest flow via fractures.

c) The cumulative discharge at the subsurface tunnel drip sites over the recharge season was between 10 and 28 times greater than the cumulative soil drainage input at the surface, indicating that flow pathways converge resulting in flow focussing at depth in the unsaturated zone. This is consistent with the inhomogeneous distribution of flow entering the tunnel. Flow convergence is thought to occur dominantly in the top 15 m of the unsaturated zone and leads to the development of solutionally enlarged pipe-like features and voids that dominate flow, as observed in the tunnel at 30 – 45 m depth.

d) The results of this study have major implications for contaminant transport and groundwater flooding. The existence of highly focussed fracture flow between the soil surface and the inflow sites in the subsurface tunnel suggests that contaminants from the surface could rapidly reach the water table even through thick unsaturated zones of the Chalk. Soil drainage events in response to high rainfall during the recharge season could therefore result in the rapid onset of water table rise and lead to groundwater flooding. The improved understanding of the short time scale flow processes and the nature of fracture controlled flow in the unsaturated zone of the Chalk resulting from this study will help to better inform future simulations and predictions of such phenomena.

Acknowledgments

The authors would like to thank Vincent Van Walt and Yvonne Coonan of Van Walt Limited who helped with the design and installation of soil monitoring instrumentation. Technical support and assistance with data interpretation was provided by Simon Bottrell and Pippa Chapman of the University of Leeds, Manoj Menon of the University of Sheffield, Rolf Farrell of the UK Environment Agency and Gerd Cachandt of Ove Arup Ltd. The manuscript was significantly improved following the comments of Andrew Ireson and two anonymous reviewers and their input is gratefully acknowledged. This work would not have been possible without the kind cooperation of landowners and the help of field assistants, notably Nicolas Barrouillet. This project was funded by the Marie Curie Initial Training network (IMVUL: Towards improved groundwater vulnerability assessment) under EU Framework 7 (Grant agreement 212298). Metrological data were provided by the UK Meteorological Office.

References

Allen, D.J., Brewerton, L.J., Coleby, L.M., Gibbs, B.R., Lewis, M.A., MacDonald, A.M., Wagstoff, S.J., Williams, A.T., 1997. The physical properties of major aquifers in England and Wales. British Geological Survey Report WD/97/34, Environment Agency R&D Publication, 8.

Allshorn, S. J. L., 2008. Flow and solute transport in the unsaturated zone of the Chalk in East Yorkshire. In Unpublished, PhD Thesis, edited, The University of Leeds.

Allshorn, S. J. L., Bottrell, S. H., West, L. J., Odling, N. E., 2007. Rapid karstic bypass flow in the unsaturated zone of the Yorkshire chalk aquifer and implications for contaminant transport. The Geological Society of London, Special Publications, 279, 111-122.

Barker, J. A., Foster S. S. D., 1981. A diffusion exchange model for solute movement in fissured porous rock. Q. J. eng. Geol. London 14, 17-24.

Barker, J. A., 1993. Modelling groundwater flow and transport in the Chalk. In: Downing, R. A., Price, M., Jones, G. P. (Eds.), The Hydrogeology of the Chalk of North-West Europe. Clarendon Press, Oxford.

Bell, F.G., Culshaw, M.G., Cripps, J.C., 1999. A review of selected engineering geological characteristics of English Chalk. Engineering Geology, 54, 237-269.

Bloomfield, J. P., 1996. Characterisation of hydrogeologically significant fracture distributions in the Chalk: an example from the Upper Chalk of southern England. Journal of Hydrology, 184(3-4), 355-379.

Bloomfield, J.P., Barker, J.A., Robinson, N., 2005. Modeling fracture porosity development using simple growth laws. Ground Water, 43, 314-326.

Bodvarsson, G.S., Wu, Y-S., Zhang, K., 2003. Development of discrete flow paths in unsaturated fractures at Yucca Mountain. Journal of Contaminant Hydrology, 62, 23-42.

Brenchley, P. J., Rawson, P. F. E., 2006. The geology of England and Wales. 2nd ed. ed., 156-156 pp., Geological Society of London, Bath.

Carsel, R. F., Parrish, R. S., 1988. Developing joint probability distributions of soil water retention characteristics. Water Resources Research, 24, 755-769.

Foster, S. S. D., Milton, V. A., 1974. The permeability and storage of an unconfined Chalk aquifer. Hydrological Sciences Bulletin, 19, 485-500.

Gale, I., Rutter, H., 2006. The Chalk aquifer of Yorkshire. British Geological Survey, Nottingham.

Geake, A. K., Foster, S. S. D., 1989. Sequential isotope and solute profiling of the unsaturated zone of the British Chalk. Hydrological Sciences Journal, 34, 79-95.

Hanna, R.B., Rajaram, H. 1998. Influences of aperture variability on dissolution growth of fissures in karst formations. Water Resources Research, 34, 2843-2853.

Hartmann, S., Odling, N. E., West, L. J., 2007. A multi-directional tracer test in the fractured Chalk aquifer of E. Yorkshire, UK. Journal of Contaminant Hydrology, 94, 315-331.

Headworth, H. G., 1972. The analysis of natural groundwater fluctuations in the chalk of Hampshire. J. Inst. Water Eng., 26, 107-124.

Hodnet, M. G., Bell, J. P., 1990. Processes of water movement through a chalk coombe deposit in Southeast England. Hydrological Processes, 4 (4), 361-372.

Holcombe, R., 2008. GEOrient 9.4.0. Edited, Department of Earth Sciences, University of Queensland, Australia.

Ireson, A. M., Butler, A.P., 2011. Controls on preferential recharge to Chalk aquifers. Journal of Hydrology, 398(1-2), 109-123.

Ireson, A. M., Mathias, S. A., Wheater, H. S., Butler, A. P., Finch., 2009. A model for flow in the Chalk unsaturated zone incorporating progressive weathering. Journal of Hydrology, 365, 244-260.

Ireson, A. M., Wheater, H. S., Butler, A. P., Mathias, S. A., Finch, J., Cooper, J. D., 2006. Hydrological processes in the Chalk unsaturated zone - Insights from an intensive field monitoring programme. Journal of Hydrology, 330(1-2), 29-43.

Lee, L. J. E., Lawrence, D. S. L., Price, M., 2006. Analysis of water-level response to rainfall and implications for recharge pathways in the Chalk aquifer, SE England. Journal of Hydrology, 330(3-4), 604-620.

Jensen, D. T., Hargreaves, G. H., Temesgen, B., Allen, R. G., 1997. Computation of Eto under nonideal conditions. Journal of Irrigation Drainage, 123(5), 394-400.

Mathias, A. S., Butler, A. P., Jackson, B.M., Wheater, H.S., 2006. Transient simulations of flow and transport in the Chalk unsaturated zone, Journal of Hydrology, 330, 10-28.

Mualem, Y., 1976. A new model predicting the hydraulic conductivity of unsaturated porous media. Water Resources Research, 12, 513-522.

National Soil Resources Institute, 2009. Academic Soils Site Report for location 495778E, 433625N, 1km x 1 km. National Soil Resources Institute, Cranfield University. Accessed via https://www.landis.org.uk/sitereporter/.

Neuman, S. P., 1987. Stochastic continuum representation of fractured rock permeability as an alternative to the REV and fracture network concepts. Proceedings 28th US Symposium on Rock Mechanics, Tucson, USA, 533-561.

Price, M., Bird, M. J., Foster, S. S. D., 1976. Chalk pore-size measurements and their significance. Water Services, 80 (968), 596-600.

Price, M., Downing, R. A., Jones, G. P., editors, 1993. The hydrogeology of the Chalk of north-west Europe, Clarendon Press, Oxford (United Kingdom).

Rowell, D. L., 1994. Soil science: methods and applications. Pearson Education Limited, Great Britain.

Scanlon, B., Healy, R., Cook, P., 2002. Choosing appropriate techniques for quantifying groundwater recharge. Hydrogeology Journal, 10(1), 18-39.

Simunek, J., Sejna, M., Saito, H., Sakai, M., van Genuchten, M. Th., 2008. The Hydrus-1D software package for simulating the movement of water, heat, and multiple solutes in variably saturated media, Version 4.0, HYDRUS Software Series 3, Department of Environmental Sciences, University of California Riverside, Riverside, California, USA, pp. 315.

Smith, D. B., Wearn, P. L., Richards, H. J., Rowe, P. C., 1970. Water movement in the unsaturated zone of high and low permeability using natural tritium. Isotope Hydrology, 73-87.

Soil Survey Staff., 2010. Keys to Soil Taxonomy, 11th ed. USDA-Natural Resources Conservation Service, Washington, DC.

van Genuchten, M. T., 1980. A closed-form equation for predicting the hydraulic conductivity of unsaturated soils. Soil Sci. Soc. Am. J., 44(5), 892-898.

Wellings, S. R., 1984. Recharge of the Upper Chalk aquifer at a site in Hampshire, England: 2. Solute Movement. Journal of Hydrology, 69(1-4), 275-285.

West, L. J., Truss, S.W., 2006. Borehole time domain reflectometry in layered sandstone: Impact of measurement technique on vadose zone process identification. Journal of Hydrology, 319, 143-162.

Figure Captions

Vadose Zone Journal Accepted Paper, posted 05/14/2012 doi:10.2136/vzj2011.0146

Figure 1. a) The Chalk outcrop in England and location of the field site; b) Cross-section of the field site indicating the location of the subsurface tunnel drip monitoring, soil core sampling, soil zone monitoring sites. The base of the Chalk is at approximately zero mASL at this location.

Figure 2. Soil profile pit at soil coring site F3 (soil monitoring installation pit).

Figure 3. Equal area stereographic projection of fracture poles showing a conjugate fracture set and the mean principal orientation of each set (GEOrient 9.4.0., Holcombe (2008)) based on 128 non-stratabound fracture orientations measured in the subsurface tunnel exposure.

Figure 4. Soil monitoring site above the subsurface tunnel indicating the installation design and position of soil monitoring probes.

Figure 5. Subsurface tunnel drip monitoring unit.

Figure 6. Time series rainfall (a) moisture content (b) and matric potential (c) at the soil plot monitoring site along with subsurface discharge at tunnel drip collector D1 (d) D2 (e) and D3 (f) over the 2009/2010 hydrological year (01-Oct 2009 to 30-Sep 2010).

Figure 7. Times series rainfall and ETp (a), HYDRUS simulated moisture content along with observed data (b), HYDRUS simulated matric potential along with observed data (c and d), HYDRUS simulated soil drainage at 1 m depth (e) and subsurface discharge at D1, D2 and D3 (f) over the winter recharge season simulation period (01-Dec 2009 to 15-Mar 2010).

doi:10.2136/vzj2011.0146

Figure 8. Observed soil moisture characteristic (SMC) curve along with the HYDRUS simulated curve at 0.45 m depth.

Figure 9. HYDRUS simulated drainage flux from 1 m depth at the soil plot monitoring site along with subsurface discharge at D1, D2 and D3. a) Peak P1and response at D2 and D3; b) Peak P1 and response at D1; c) Peak P2 and response at D1 and D2; d) Peak P2 and response at D1; e) Peak P3 and response at D2 and D3; and f) Peak P3 and response at D1.

Figure 10. Conceptualization of recharge season flow convergence in the Chalk unsaturated zone via solutionaly enlarged fracture pathways showing the development of major convergence in the top 15 m.

 doi:10.2136/vzj2011.0146

Tables

Table 1. Moisture content, dry bulk density and porosity values from soil zone core samples

Core extraction site:		F1 –field peas			F2 –grazed perm. grassland			F3 –winter wheat			
Sample date:		03.2010			11.2010			03.2010			
Type	Sample Depth (m)	MC (% Vol)	DBD (kg/m^3)	Por. (%)	MC (% Vol)	DBD (kg/m^3)	Por. (%)	TDR (%)	MC (% Vol)	DBD (kg/m^3)	Por. (%)
Soil	0 – 0.25	18.7	1360	49	31.8	1590	40	-	29.7	1340	49
Soil	0.25 – 0.40	17.8	1460	45	24.7	1750	34	27 †	29†	1420†	47†
Chalk	0.60	31.2	1660	39	35.6	1770	35	30	23	1660	39
Chalk	0.80	19	1610	41	-	-	-	27.5	26.5	1640	39

MC = moisture content, DBD = dry bulk density, Por. = porosity, TDR = Logged TDR probe measurement at F3 –measurement at 0.25 - 0.4 m depth in table is TDR point measurement at 0.4 m, †09.2010.

Table 2. Final soil hydraulic input parameters for HYDRUS simulated drainage flux

Layer	classification	Depth (m)	θ_r (% Vol)	θ_s (% Vol)	α (mm)	n	K_s (mmhr^{-1})
1	Silty clay loam	0.0 - 0.3	5	45	0.001	3.08	420
2	Silty clay loam and highly weathered chalk	0.3 – 0.6	5	29	0.016	1.04	720
3	Highly weathered chalk	0.6 – 1.0	9	35	0.191	1.05	8130

 doi:10.2136/vzj2011.0146

Table 3. Cumulative soil drainage estimate and tunnel discharge over the winter recharge season (1 December 2009 - 15 March 2010 (2520 hrs))

Input	Cumulative rainfall:			206 mm	
	Cumulative soil drainage estimate (1 m depth)			168 mm	
Subsurface Discharge	Location	Depth (m)	Fracture spacing (m)	Cumulative discharge (mm)	Estimated catchment area (m^2)
	D1	45 m	4.6	4648‡	28
	D2	45 m	9.2	1643	10
	D3	30 m	7.1	3348	20

‡ Corrected from measured cumulative total (3254 mm) which was missing 758 hrs data

Table 4. Mean hydraulic response times at D1, D2 & D3 to peak soil drainage events (P1, P2 and P3)

Hydraulic response	P1 – P3	D1	D2	D3
Mean peak lag time (hr)	-	112 (4.6 days) (range: 99 – 125)	23 (<1 day) (range: 18 – 27)	15 (<1 day) (range: 11 – 18)
Mean event duration (hr)	24 (1 day) (range: 12-32)	376 (15.6 days) (based on 1 event)	50 (~2 days) (range: 34 – 64)	125 (~5 days) (range: 96 – 166)
Mean extension ratio	-	188 (based on 1 event)	20 (range: 4 – 32)	48 (range: 14 – 83)

 doi:10.2136/vzj2011.0146

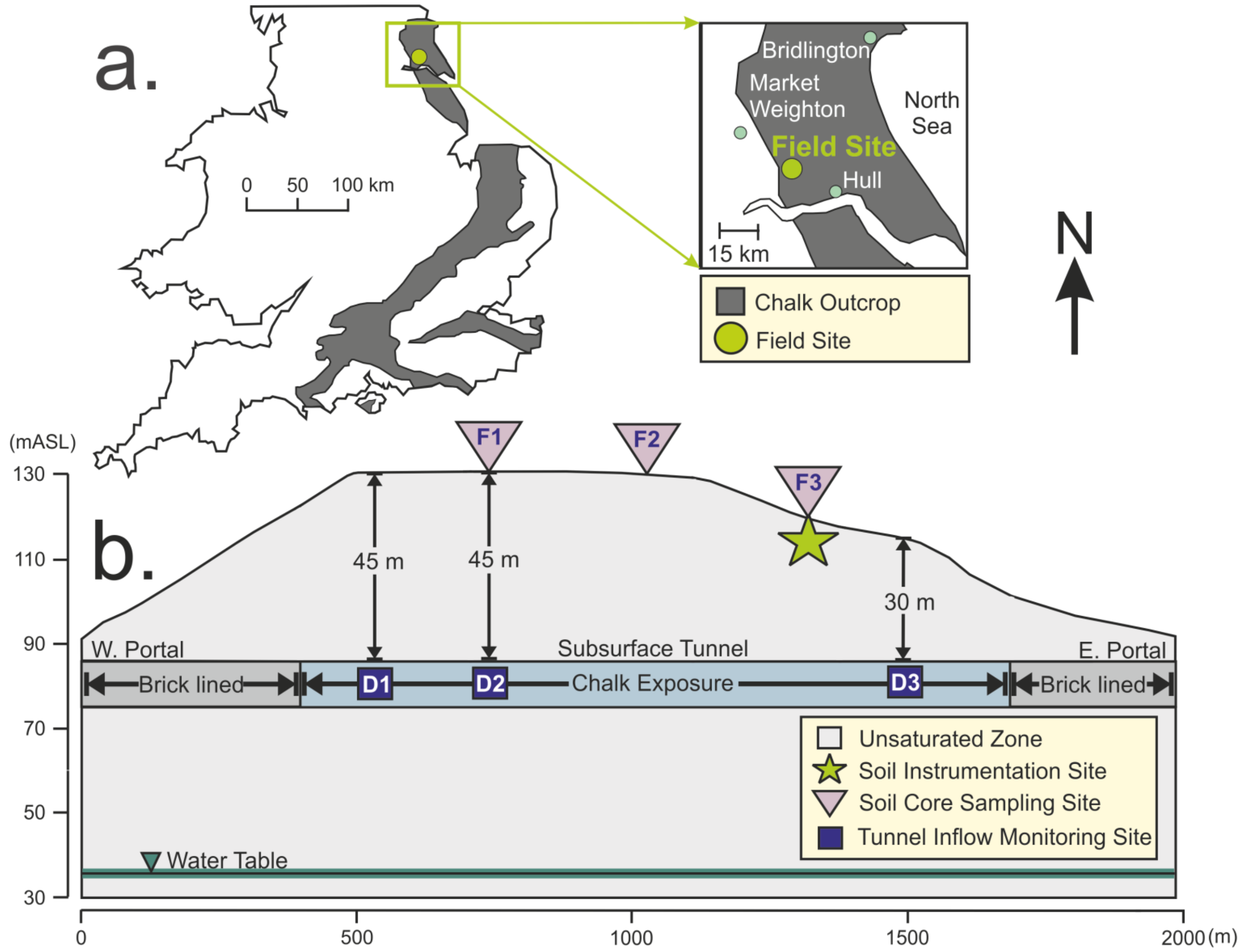

Fig. 1

 doi:10.2136/vzj2011.0146

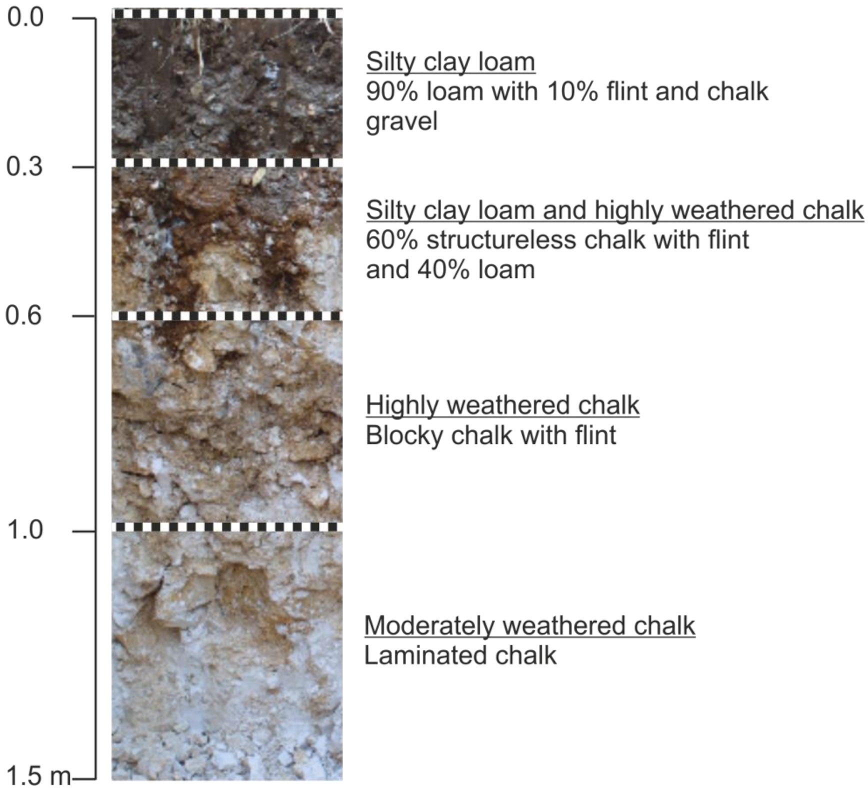

Fig. 2

 doi:10.2136/vzj2011.0146

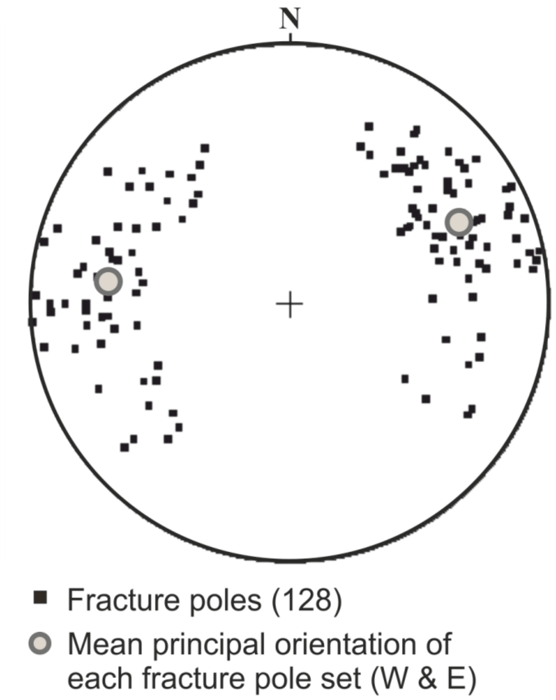

Fig. 3

doi:10.2136/vzj2011.0146

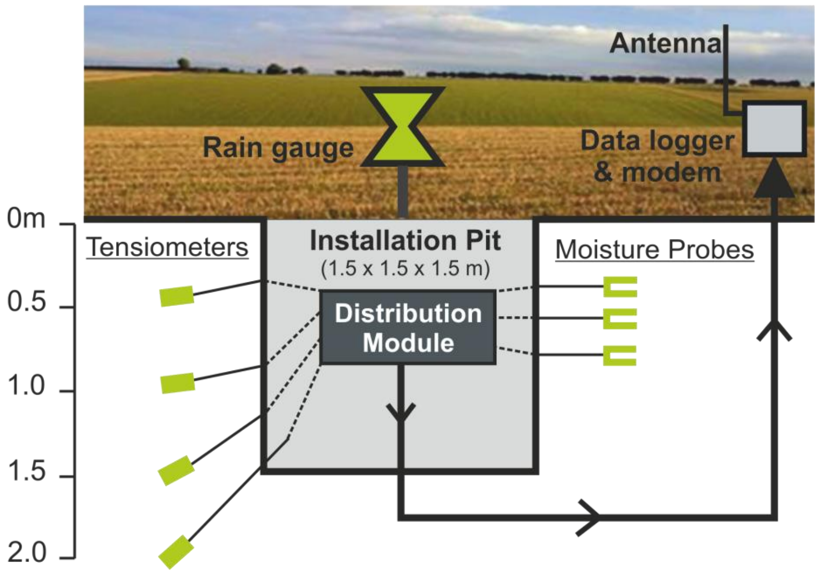

Fig. 4

 doi:10.2136/vzj2011.0146

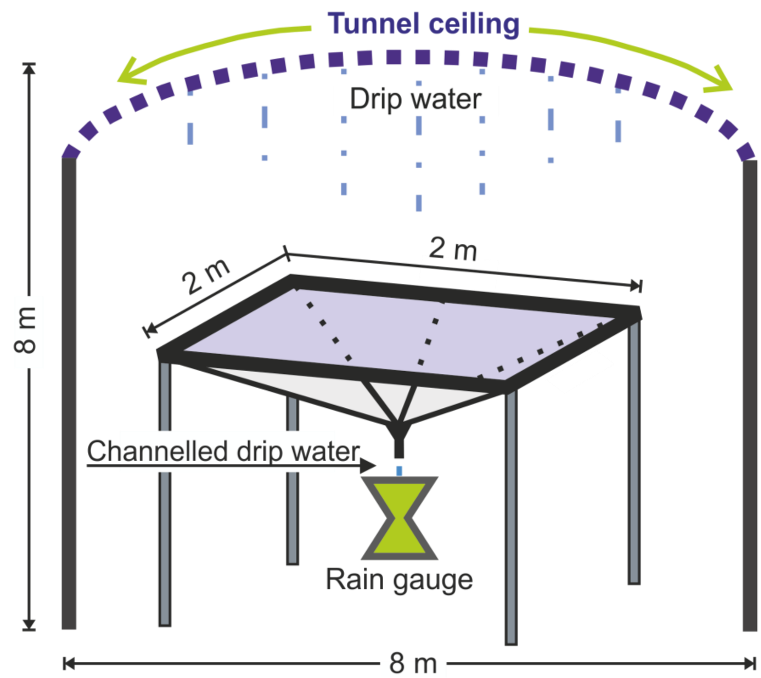

Fig. 5

 doi:10.2136/vzj2011.0146

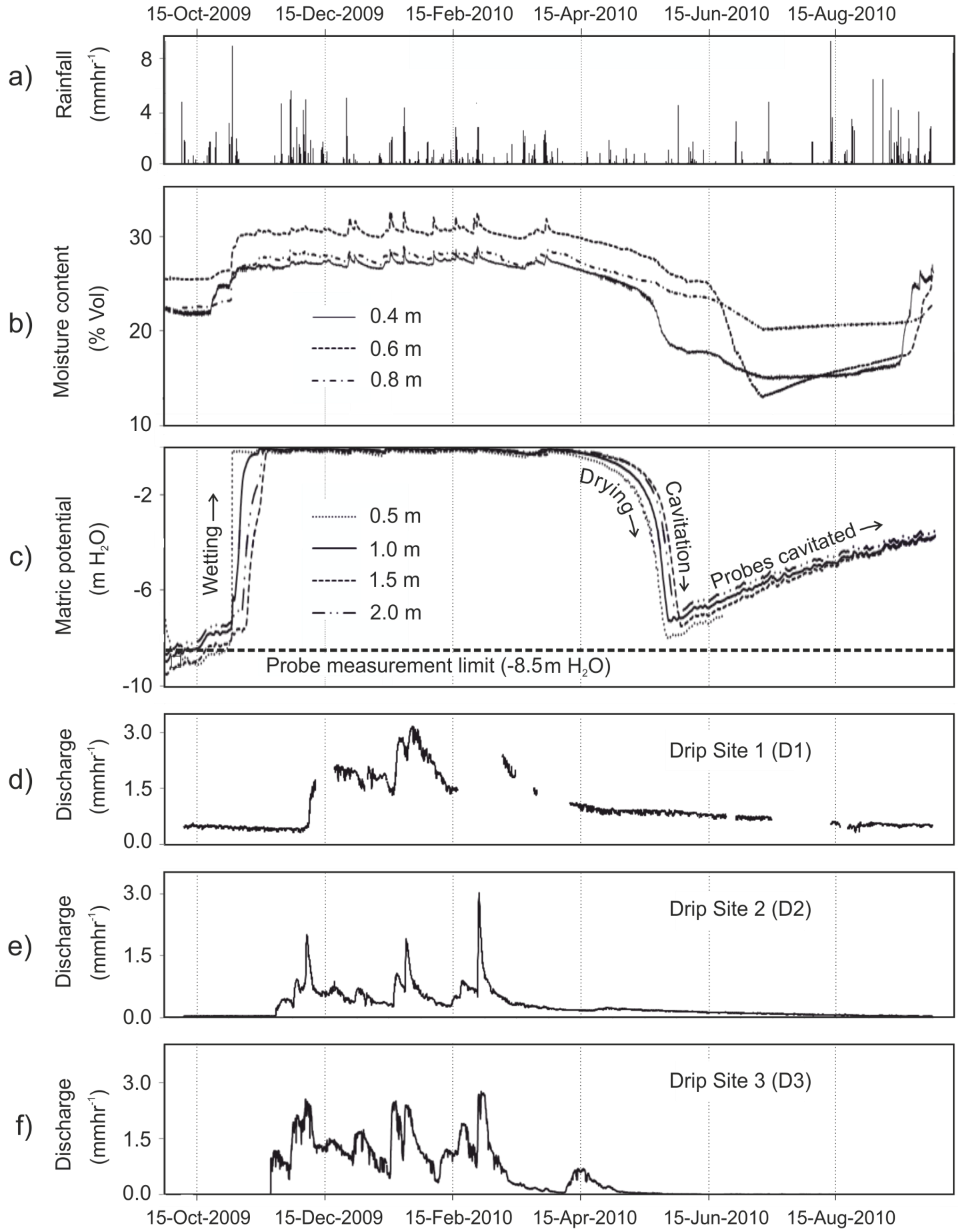

Fig. 6

 doi:10.2136/vzj2011.0146

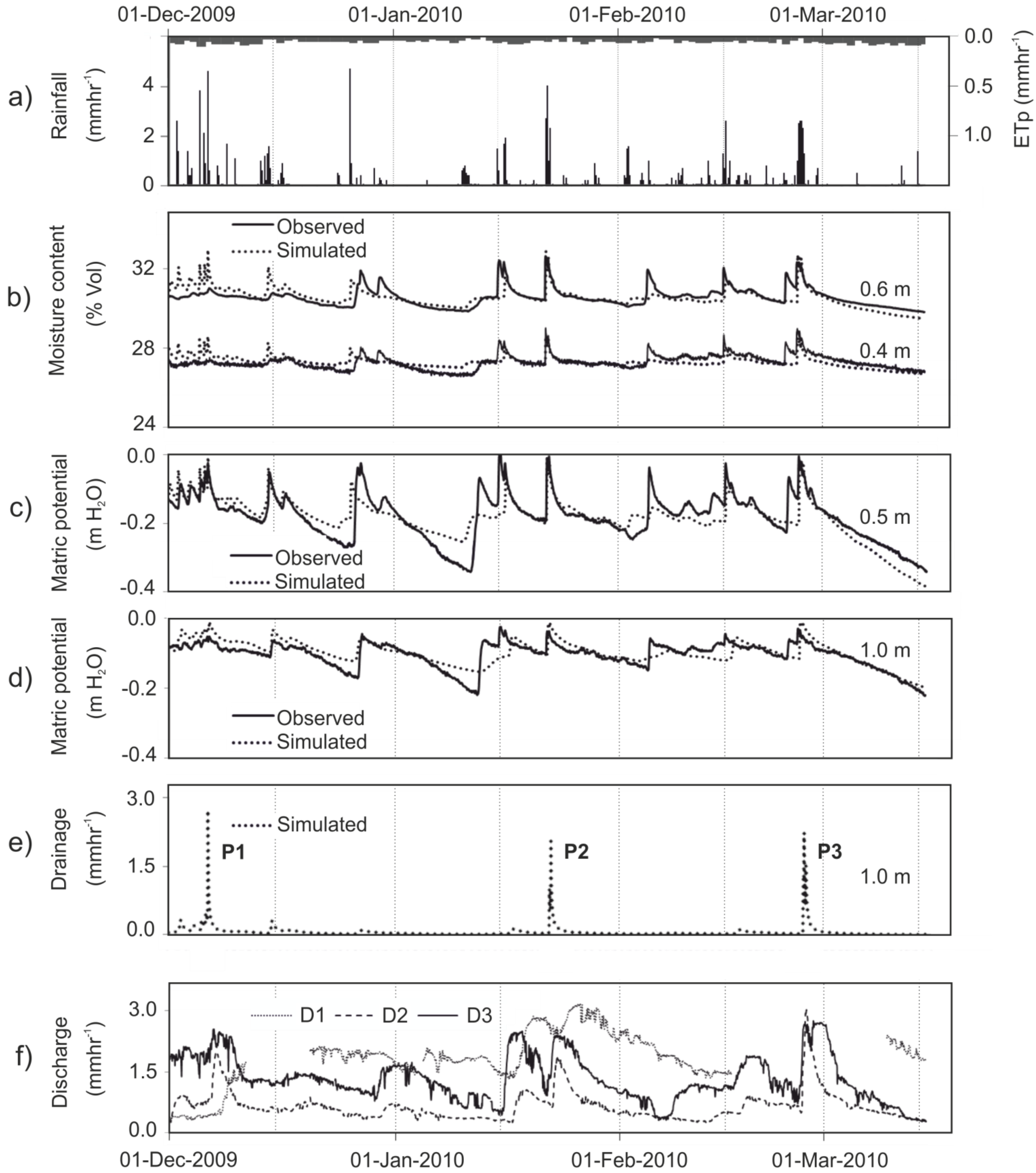

Fig. 7

doi:10.2136/vzj2011.0146

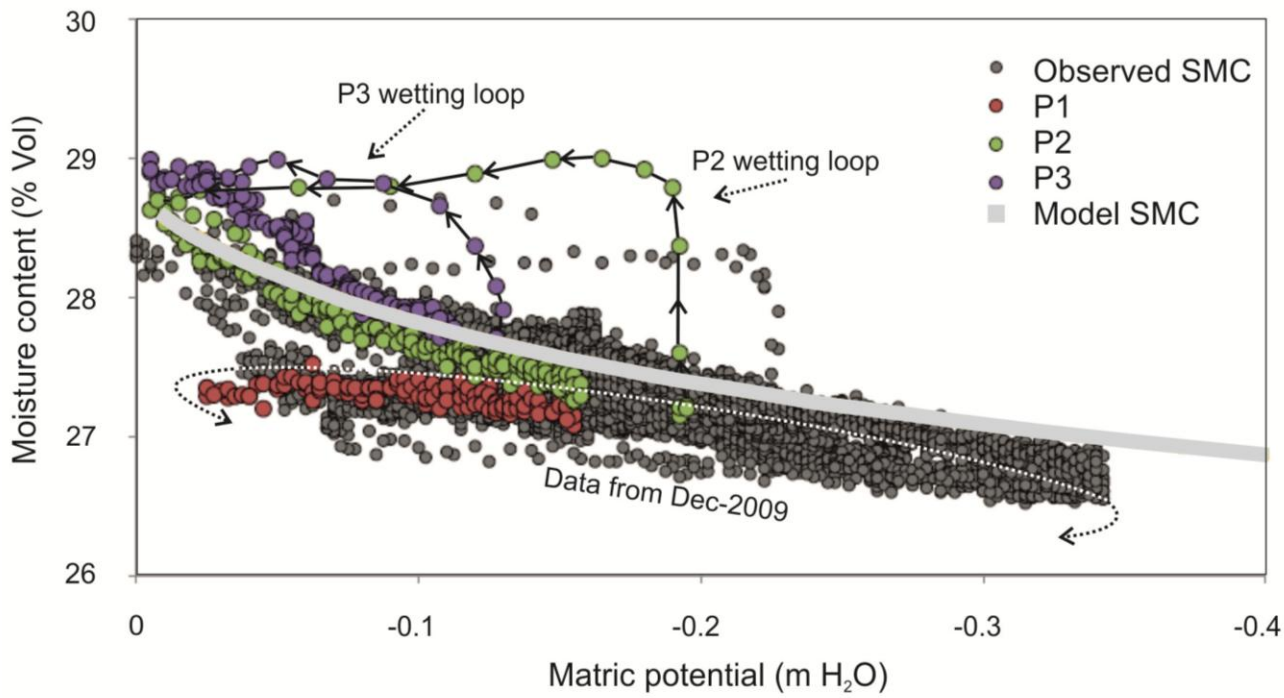

Fig. 8

 doi:10.2136/vzj2011.0146

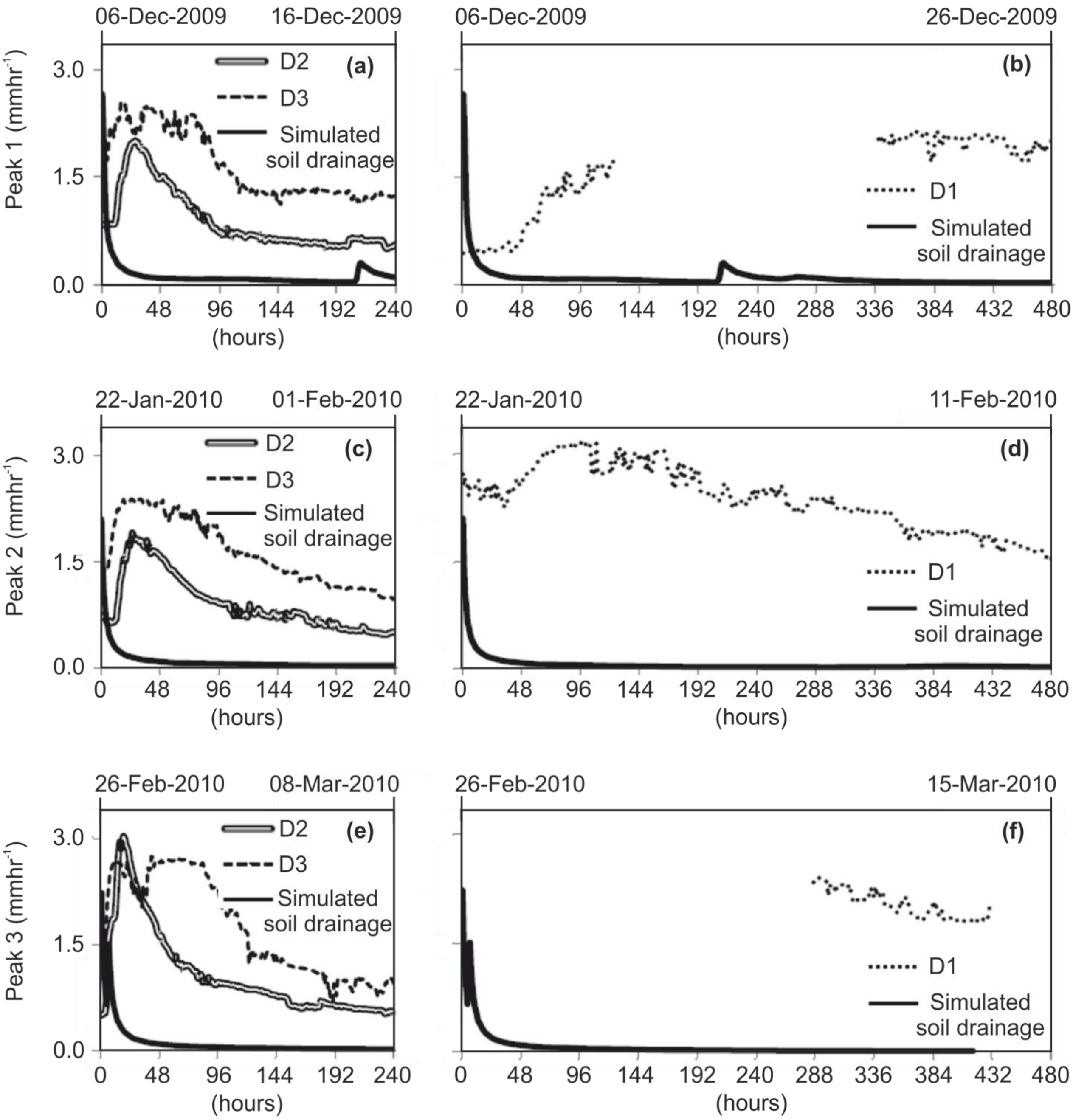

Fig. 9

doi:10.2136/vzj2011.0146

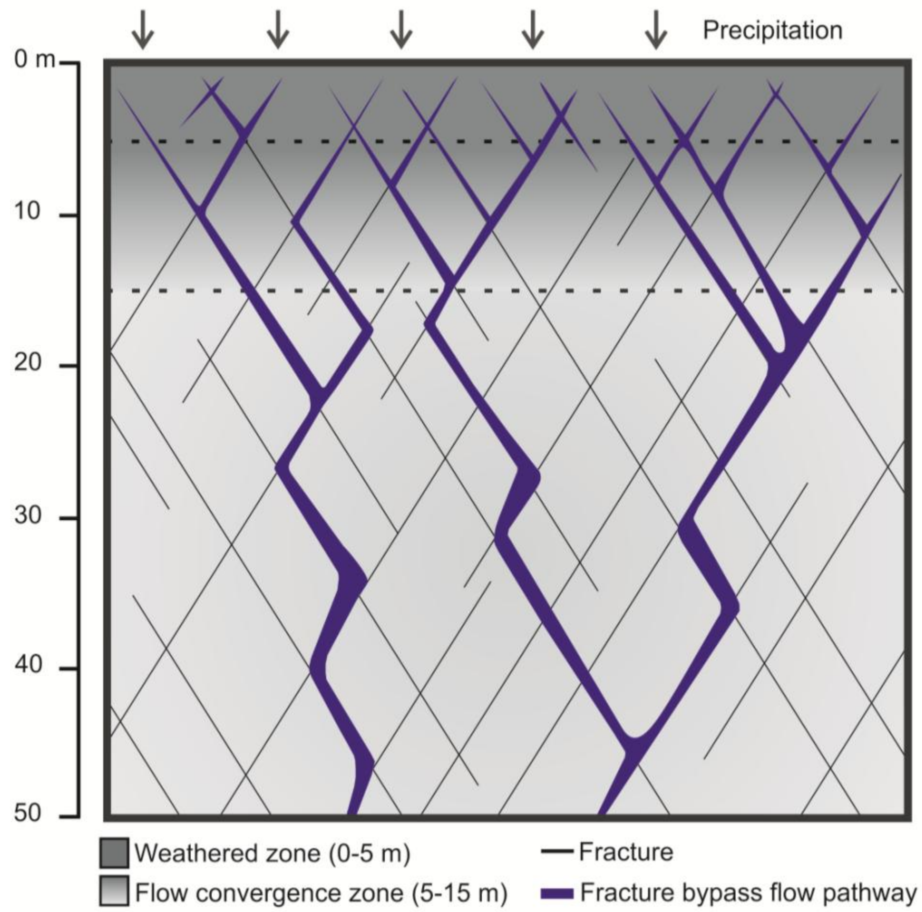

Fig. 10